

Microwave Pulse Propagation inside a 3D Heart Model

L. Nickelson, S. Ašmontas,

Semiconductor Physics Institute, A. Gostauto str. 11, LT-01108 Vilnius, Lithuania, tel.: +370 5 2792951, +370 5 2619759, fax: +370 5 2627123, e-mail: lucynickelson@gmail.com, asmontas@pfi.lt

R. Martavičius

Electronic Systems Department, Electronics Faculty, Vilnius Gediminas Technical University, Naugarduko str. 41, LT-03227 Vilnius, Lithuania, tel.: +370 5 2744765, fax: +370 5 2744770, e-mail: romanus.martavicius@el.vtu.lt

V. Engelson

Linköping university,

SE-58183, Linköping, Sweden, tel.: 46 13 281979, fax: 46 13 284499, e-mail: vaden@ida.liu.se

Introduction

For the past two decades research on the medical effects of the influence of microwaves on different biological systems has increased greatly. The main reason for the increased interest is because of the vast amount of man-made microwave fields in the environment around the world. At the present time it is especially important in studying the influence of modulated microwaves on living organisms because microwaves are used in many telecommunication devices such as cell phones and radio transmitters [1-6].

In article [1] it was explained that current mobile radio applications have a modulating signal frequency range of several Hertz to several Kilohertz. TETRA (Terrestrial Trunked Radio) mobile equipment employs a modulating signal with a frequency of 17.65 Hz. Some biological processes run on timescales that extend from a very short period of time up to very long periods of time although some have time constants similar to the pulse duration of different electronic equipment.

In article [2] the influence of the continuous (CW) and pulsed (PW) microwaves at 2.45 GHz on different parts of human and animal body were analysed. There was a greater increase in the skin temperature around the area facing the antenna during PW exposure than during CW exposure.

Article [3] shows a relatively large thermal gradient exists during exposure of animals to microwaves particularly at high frequencies. The article describes the effects of short and extremely high power microwave pulses (EHPP) on neuronal network functions. The EHPP carrier frequency was 9.3 GHz, the pulse width and repetition rate were from 0.5 to 2 μ s and from 0.5 to 10 Hz, respectively. The authors did not observe delayed or lasting effects of EHPP.

In article [4] they investigated different brain characteristics when pulse-modulated frequencies were decreased from 500 to 250 pulses per second. A comparison of the effects of continuous-wave, sinusoidal-amplitude-modulated, and pulsed square-wave-modulated microwave exposures on brain energy metabolism were made.

Article [5] described the effects of two types of pulse-modulated electromagnetic fields on regional cerebral blood flow in 12 healthy young men. The two types of microwave exposure were: a "base-station-like" and a "handset-like" signal.

Article [6] focused on the effect of low level microwave radiation on human EEG alpha (7.5-12.5 Hz) and theta (3.5-7.5 Hz) rhythms. During the experiment, 20 healthy volunteers were exposed to microwaves with 7 Hz on-off modulation. The experimental results demonstrated that microwave stimulation effects became apparent, starting from the third stimulation cycle.

Scientific papers analyse microwave problems in very diverse ways but most of them are devoted to experimental investigations only. These investigations are carried out by dosimeters and spectroscopy issues on cultured cells, isolated organs, animals and humans. The influence of microwaves on living organisms can produce various phenomena.

In article [7] the participants' cognitive performance was impaired after exposure to pulsed electromagnetic fields. In [8]–[10] microwave exposure was shown to stimulate tissue repair, regeneration, relieved stress and facilitated recovery in animals and humans. It is important to research these phenomena which are dependent on frequencies, waveforms, amplitude of microwaves and other parameters.

In this present article our numerical investigations are devoted to the influence of microwave pulses on a three-

dimensional (3D) heart model. In our previous articles [11], [12] we analysed the microwave electric field distribution of a 3D heart model depending on the shape and location of a microwave catheter which was placed inside of it. In article [13] we analysed the scattered electric field on a 3D heart model. The heart model was illuminated by an incident vertically and horizontally polarized plane microwave from an external point source.

SIE method for microwave fields analyses inside a 3D heart model

We formulated our electrodynamic problem like this: an antenna radiates a microwave pulse into a 3D heart model (Fig. 1). The heart model has an intricate shape. An antenna is placed outside the heart model touching it.

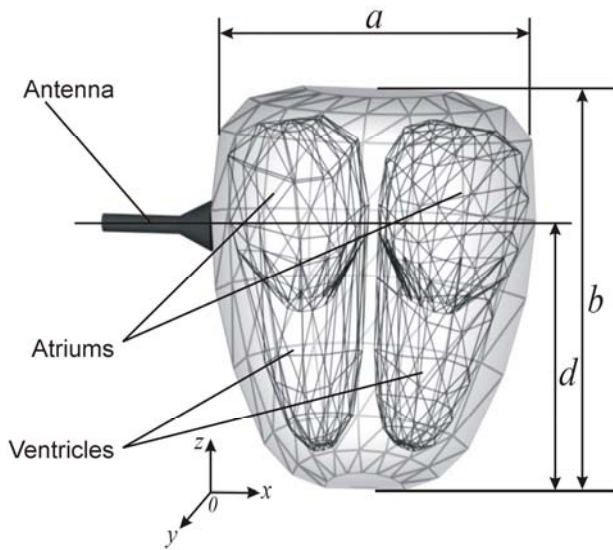


Fig. 1. The heart model with the myocardium, the left and right atriums and ventricles used in calculations

We assumed the monochromatic carrier microwave with an angular frequency ω_0 was modulated with a video pulse. Mathematically we presented the monochromatic carrier microwave with a harmonic cosine function $\cos(\omega_0 t)$. We solved an electrodynamic problem for two types of modulating signals. The first modulating signal was a triangular video pulse and the second modulating signal was a rectangular video pulse. We calculated for two values of the on-off time ratio T/τ .

The pulse durations τ were always equal to 20 ms. The magnitudes of the pulse period T were different in our calculations. The magnitude of the pulse duration was chosen in order to be equal to the duration of a triangular pick “QRS” of human cardiograms [14].

In this article we presented the algorithm that is based on the singular integral equations (SIE) method, which allowed us to carry out numerical investigations of an electric field distribution into a 3D heart model (Fig.1). The surface of the 3D heart model as well the antenna was created in the 3D Studio MAX. This tool exports the

surfaces as a set of triangles with a normal vector on certain surface points.

The heart model consisted of cardiac muscle and the right and left atriums with ventricles cavities which were filled with blood. The width a of this model was 9 cm, the length b was 13 cm and distance $d=9$ cm. Here we assumed that the antenna was made of ideal metal and radiated a microwave pulse. We also assumed that a microwave point source was placed at the tip of the antenna.

To present the field in integral form for this electrodynamic problem we used the solution to Maxwell’s equations with electric and magnetic point sources:

$$\begin{cases} \text{rot } \vec{H} = i\omega\epsilon_0\epsilon\vec{E} - \vec{j}_e, \\ \text{rot } \vec{E} = i\omega\mu_0\mu\vec{H} - \vec{j}_m. \end{cases} \quad (1)$$

Because of the linearity the general solution is the sum of solutions for $\vec{j}_e \neq 0, \vec{j}_m = 0$ and $\vec{j}_e = 0, \vec{j}_m \neq 0$. The first is called an electric wave and the second is called a magnetic wave.

The solution to Maxwell’s equations (1) is constructed as a superposition of hybrid quasi-E and quasi-H waves. In our SIE method we separated the solution of equations from satisfying the boundary conditions. In the beginning we found the solution of the differential equations having a δ -function on the right side, i.e. the solution to the point source problem. Then this fundamental solution is used in the integral representation of an electromagnetic field for solving an electrodynamic problem of an arbitrarily shaped 3D body, which can be characterized by a set of the complex dielectric permittivities. The electric field representation is

$$\begin{aligned} \vec{E}(\vec{r}_1) = & \int_{S_i} \mu_e(\vec{r}_0) \left\{ \frac{1}{k^2 \epsilon_p \mu_p} \nabla(\vec{n}(\vec{r}_0), \nabla) + \vec{n}(\vec{r}_0) \right\} \times \\ & \times h_0 \left(k\sqrt{\epsilon_p \mu_p} |\vec{r}_1 - \vec{r}_0| \right) dS - \\ & - jZ_0 \sqrt{\frac{\mu_p}{\epsilon_p}} \int_{S_i} \mu_m \left[\vec{n}(\vec{r}_0), \frac{\vec{r}_1 - \vec{r}_0}{|\vec{r}_1 - \vec{r}_0|} \right] \times \\ & \times h_1 \left(k\sqrt{\epsilon_p \mu_p} |\vec{r}_1 - \vec{r}_0| \right) dS \end{aligned} \quad (2)$$

and the magnetic field representation is:

$$\begin{aligned} \vec{H}(\vec{r}_1) = & \frac{j}{Z_0} \sqrt{\frac{\epsilon_p}{\mu_p}} \int_{S_i} \mu_m(\vec{r}_0) \left[\vec{n}(\vec{r}_0), \frac{\vec{r}_1 - \vec{r}_0}{|\vec{r}_1 - \vec{r}_0|} \right] \times \\ & \times h_1 \left(k\sqrt{\epsilon_p \mu_p} |\vec{r}_1 - \vec{r}_0| \right) dS + \\ & + \int_{S_i} \mu_e(\vec{r}_0) \left\{ \frac{1}{k^2 \epsilon_p \mu_p} \nabla(\vec{n}(\vec{r}_0), \nabla) + \vec{n}(\vec{r}_0) \right\} \times \\ & \times h_0 \left(k\sqrt{\epsilon_p \mu_p} |\vec{r}_1 - \vec{r}_0| \right) dS. \end{aligned} \quad (3)$$

Here unknown functions $\mu_e(\vec{r}_0)$ and $\mu_m(\vec{r}_0)$ respectively are electric and magnetic source densities in the point \vec{r}_0 on the surface of the 3D heart model. The quantity $|\vec{r} - \vec{r}_0|$ is the distance from the point \vec{r} where we want to determine the fields $\vec{E}(\vec{r}_1)$ and $\vec{H}(\vec{r}_1)$ to the electric and magnetic source densities ($\mu_e(\vec{r}_0)$ and $\mu_m(\vec{r}_0)$) in the point \vec{r}_0 . The quantity $\vec{n}(\vec{r}_0)$ is a unit normal vector to the surface at the same point. The quantity $k = 2\pi/\lambda$ is the wave number and λ is the wavelength of the monochromatic carrier microwave which propagates in free space. The quantity $Z_0 = \sqrt{\mu_0/\varepsilon_0}$ is the characteristic impedance of the free space. We assumed in this article that the permittivities ε_p and permeabilities μ_p of the heart tissue and the surrounding areas are scalars, where indexes $p=1, 2, 3$ represent the cardiac muscle, the blood, and free space respectively. So magnitudes $\hat{\varepsilon}_p = \varepsilon'_p - j\varepsilon''_p$ and $\mu_p = 1$ represent the relative permittivity and permeability for the cardiac muscle, the blood and free space. The function $\beta_0 = h_0(k\sqrt{\varepsilon_p\mu_p}|\vec{r} - \vec{r}_0|)$ is the spherical Hankel function of the zeroth order and the second kind. The function $\beta_1 = h_1(k\sqrt{\varepsilon_p\mu_p}|\vec{r} - \vec{r}_0|)$ is the spherical Hankel function of the first order and the second kind. The value dS is an infinitesimal patch of area. The sign $\nabla = \vec{i}\frac{\partial}{\partial x} + \vec{j}\frac{\partial}{\partial y} + \vec{k}\frac{\partial}{\partial z}$ is the gradient operator and $j = \sqrt{-1}$. In the formulae the notations

$$S = (\vec{n}(\vec{r}_0), \nabla), \quad S_0 = \left(\vec{n}(\vec{r}_0), \frac{\vec{r}_1 - \vec{r}_0}{|\vec{r}_1 - \vec{r}_0|} \right),$$

$$S_1 = \left(\vec{n}(\vec{r}_1), \frac{\vec{r}_1 - \vec{r}_0}{|\vec{r}_1 - \vec{r}_0|} \right)$$

$$\text{vectors, } V_0 = \left[\vec{n}(\vec{r}_0), \frac{\vec{r}_1 - \vec{r}_0}{|\vec{r}_1 - \vec{r}_0|} \right], \quad V_1 = \left[\vec{n}(\vec{r}_1), \frac{\vec{r}_1 - \vec{r}_0}{|\vec{r}_1 - \vec{r}_0|} \right]$$

and $V_n = [\vec{n}(\vec{r}_1), \vec{n}(\vec{r}_0)]$ are the vector products of two vectors. Other notations are:

$$D_1 = \frac{h_1(k\sqrt{\varepsilon_p\mu_p}|\vec{r}_1 - \vec{r}_0|)}{k\sqrt{\varepsilon_p\mu_p}|\vec{r}_1 - \vec{r}_0|}, \quad (4a)$$

$$D_2 = \frac{\vec{r}_1 - \vec{r}_0}{|\vec{r}_1 - \vec{r}_0|} (\vec{n}(\vec{r}_1), \vec{n}(\vec{r}_0)), \quad (4b)$$

$$D_3 = \frac{3}{k\sqrt{\varepsilon_p\mu_p}|\vec{r}_1 - \vec{r}_0|} \cdot h_1(k\sqrt{\varepsilon_p\mu_p}|\vec{r}_1 - \vec{r}_0|). \quad (4c)$$

As an example, we will write the formula for the boundary conditions on the exterior surface of the heart that divides two mediums. One medium has parameters of free space (index $p=3$) and the other medium has parameters of the cardiac muscle (index $p=1$). Equating

the vector product $[\vec{n}(\vec{r}_1), \vec{E}(\vec{r}_1)]^+ =$
 $[\vec{n}(\vec{r}_1), \vec{E}(\vec{r}_1)]^-$ we get the integral equation:

$$\begin{aligned} & \int_{S_i} \mu_e^+(\vec{r}_0) \{ S_0 \times V_1 \times (D_3 - \beta_0) + \\ & + V_n \times (\beta_0 - D_1) \} dS - \\ & - jZ_0 \sqrt{\frac{\mu_1}{\varepsilon_1}} \int_{S_i} \mu_m^+(\vec{r}_0) \{ \vec{n}(\vec{r}_0) \times S_1 - D_2 \times \beta_1 \} dS = \\ & = [\vec{n}(\vec{r}_1), \vec{E}_{mw}(t, \vec{r}_1)]^- + \int_{S_i} \mu_e^-(\vec{r}_0) \{ S_0 \times V_1 \times \\ & \times (D_3 - \beta_0) + V_n \times (\beta_0 - D_1) \} dS - \\ & - jZ_0 \sqrt{\frac{\mu_3}{\varepsilon_3}} \int_{S_i} \mu_m^-(\vec{r}_0) \{ \vec{n}(\vec{r}_0) \times S_1 - D_2 \times \beta_1 \} dS, \quad (5) \end{aligned}$$

where in the notations of the magnitudes D_1, D_3, β_0 and β_1 the index "p" will be equal to 1 for the left part of the equation (4), and the index "p" = 3 for the right part.

Equating the vector product $[\vec{n}(\vec{r}_1), \vec{H}(\vec{r}_1)]^+ =$
 $[\vec{n}(\vec{r}_1), \vec{H}(\vec{r}_1)]^-$ for a magnetic field we received a similar integral equation as (4). The vector $\vec{E}_{mw}(t, \vec{r}_1)$ in the equation (4) is an electric field of a microwave pulse that is radiated by an antenna (Fig. 1). We assumed that the magnitude of this vector $\vec{E}_{mw}(t, \vec{r}_1)$ when the carrier microwave is modulated by triangular video pulses [15] is equal to:

$$\begin{aligned} \vec{E}_{mw\Box}(t, \vec{r}_1) &= \frac{E_0}{2q} \left[1 + 2 \sum_{k=1}^{2q} \left(\frac{\sin(\Omega_{\Box})}{(\Omega_{\Box})} \right)^2 \cos k\omega_1 t \right] \times \\ &\times \cos \omega_0 t. \quad (6) \end{aligned}$$

When the carrier microwave is modulated by rectangular video pulses [15] is equal to:

$$E_{mw\Box}(t, r_1) = \frac{E_0}{q} \left[1 + 2 \sum_{k=1}^q \left(\frac{\sin(\Omega_{\Box})}{(\Omega_{\Box})} \right)^2 \cos k\omega_1 t \right] \times \cos \omega_0 t,$$

$$\text{where } \Omega_{\Box} = \frac{k\pi}{2q}, \Omega_{\Box} = \frac{k\pi}{q}, \omega_1 = \frac{2\pi}{T}, q = \frac{T}{\tau}, \quad (7)$$

$\omega_0 = 2\pi f_0$, f_0 – the monochromatic carrier microwave frequency.

The system of SIE was reduced to an algebraic system of linear equations and this system was solved numerically.

Our calculations fulfilled by the SIE method were compared to experimental and theoretical results for simple diffraction problems from different articles. These comparisons are given in the book [16]. We believe that we can use our SIE method to study electromagnetic processes in a heart model which is under the influence a microwave pulses.

Numerical results

In our calculations the frequency of the carrier microwave was $f_0 = 10$ GHz. The magnitudes of the real and imaginary parts of the relative permittivity for the cardiac muscle $\hat{\epsilon}_1 = 80 - j5$ and the blood $\hat{\epsilon}_2 = 55 - j7$ were taken from literature [17], [18].

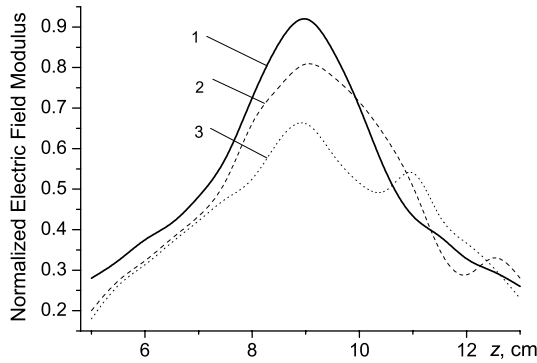


Fig. 2. Distribution of magnitude $|\vec{E}|/|\vec{E}_{\max}|$ along the z axis in three transversal cross sections with the coordinate $x = 1$ cm (curve 1), 3 cm (curve 2), 5 cm (curve 3) when a modulating signal is a triangular video pulse with the on-off time ratio $T/\tau = 3$

Figures 2–5 show the distribution of the normalized electric field modulus $|\vec{E}|/|\vec{E}_{\max}|$ at the longitudinal cross-sections along the z coordinate axis. Here the magnitude \vec{E}_{\max} is the amplitude of the microwave electric field in the center of the antenna tip and the electric field modulus

$|\vec{E}| = \sqrt{E_x^2 + E_y^2 + E_z^2}$. The microwave pulse that is radiated by an antenna (Fig. 1) is obtained when the monochromatic carrier microwave signal is modulated by video pulses. In our calculation a video pulse is formed of harmonics. Figures 2–5 show the distributions in three heart model cross-sections which are removed from the antenna tip by the distance 1 cm, 3 cm and 5 cm. Curve 1 shows the electric field distribution at the nearest cross-section to the antenna tip. We see that the electric field amplitude is the largest in the first cross-section of the heart. So the closer a cross-section to the antenna tip the larger is the amplitude of the electric field in that cross-section. In Fig. 2 and Fig. 3 we see the electric field distribution when the monochromatic carrier microwave was modulated by the triangular video pulse with a different on-off time ratio T/τ equal to three and thirty.

Fig. 2 shows that the microwave electric field amplitude changes asymmetrically to the antenna tip when the microwave pulses propagate into the heart model. It happened because the chambers of the heart model from which surfaces reflected the microwave pulse are located asymmetrically compare to the antenna tip. We see the microwave electric field distribution into the heart model cross-section at a distance of 5 cm (curve 3) undergoes the most distortion compared to the previous cross-sections (curves 1 and 2).

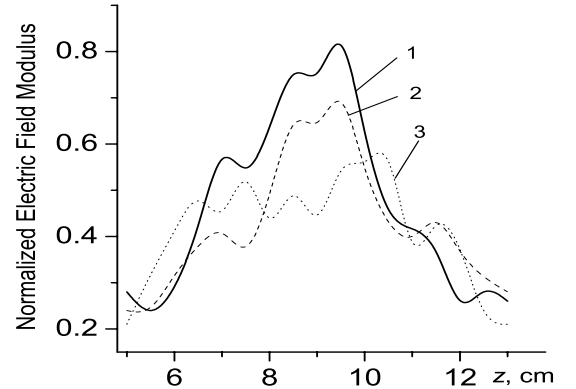


Fig. 3. Distribution of magnitude $|\vec{E}|/|\vec{E}_{\max}|$ along the z axis in three transversal cross sections with the coordinate $x = 1$ cm (curve 1), 3 cm (curve 2), 5 cm (curve 3) when a modulating signal is a triangular video pulse with the on-off time ratio $T/\tau = 30$

Analysing Fig. 2 we see that the distributions of the microwave electric field inside of the heart model are stipulated by the phenomena of the microwave pulse propagation inside of an inhomogeneous media which has a complicated shape. It is important to note five factors which determine the microwave pulse propagation: 1) the modulating signal which is a video pulse we describe by formulae (5) as a sum of harmonics; 2) a number of harmonics which approximate the modulating video pulse is chosen proportional to the on-off time ratio of the pulse; 3) a number of harmonics depends on the form of a video pulse also and we choose this number according to the

recommendations of [15]; 4) harmonics of the microwave signals can reflect repeatedly from the interior and external heart model surfaces; 5) the harmonics interference occurs inside of the heart model; 6) the media of the heart model is the cardiac muscle and blood which is the loss materials with complex dielectric permittivities and here a microwave signal can be attenuated.

When we examine curves 1-3 in Fig. 3 we see that the amplitudes of the normalized electric field modulus change and that they are more complicated compared to the same curves in Fig. 2. This happens because in our calculations (Figs. 2 and 3) a number of harmonics which approximate the modulating pulse were chosen equal to six and sixty, respectively.

In Fig. 4 and Fig. 5 we see the electric field distribution when the carrier microwave was modulated by the rectangular video pulses with a different on-off time ratio.

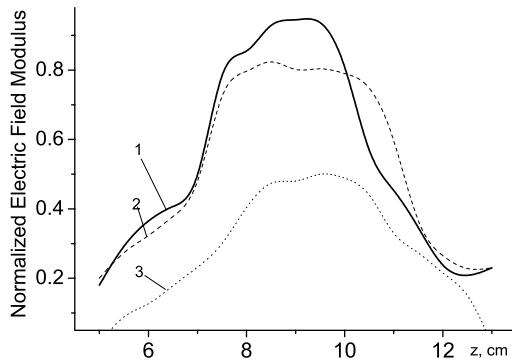


Fig. 4. Distribution of magnitude $|\vec{E}|/|\vec{E}_{\max}|$ along the z axis in three transversal cross sections with coordinates $x = 1$ cm (curve 1), 3cm (curve 2), 5 cm (curve 3) when a modulating signal is a rectangular video pulse with the on-off time ratio $T/\tau = 3$

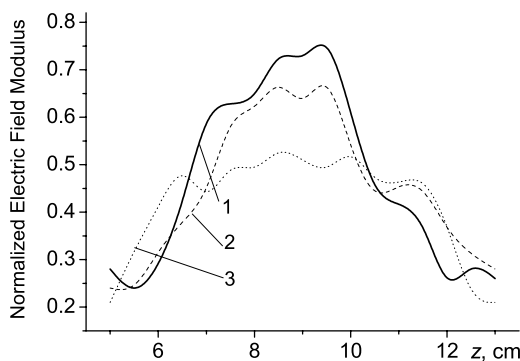


Fig. 5. Distribution of magnitude $|\vec{E}|/|\vec{E}_{\max}|$ along the z axis in three transversal cross sections with the coordinate $x = 1$ cm (curve 1), 3cm (curve 2), 5 cm (curve 3) when a modulating signal is a rectangular video pulse with the on-off time ratio $T/\tau = 3$

In the Fig. 4 and Fig. 5 we see the same distributions of the electric field in the heart cross-sections. The video pulses were formed from three and thirty harmonics in our calculations of curves Fig. 4 and Fig. 5 respectively.

The main dependencies are the same as we described before. When the microwave pulses were removed from the antenna tip the amplitude became less. When a number of harmonics increase the distribution of the electric field into the heart model became more complicated.

The authors of references [2–6] prove experimentally that the influence of modulated microwave signals on different biological systems exists. Article [1] explains this phenomenon. In order to influence the modulated microwave signals on a living organism it is necessary to demodulate this signal and it is necessary to use a non-linear element. But in biology the cell membrane fulfills the function of a non-linear element [1]. So the microwave pulse phenomenon makes it possible to create advanced microwave devices.

Conclusions

1. We used our SIE method to solve Maxwell's equations relating to the propagation of microwave pulses inside of a 3D heart model.
2. We investigated microwave electric field distributions at several cross-sections of a 3D heart model.
3. We discovered that the microwave electric field distribution strongly depends on the form and the on-off time ratio of modulating video pulses.
4. We discovered that the amplitude of the electric field decreased while the microwave pulses were moving away from the antenna tip. This happened because the 3D heart model consists of different loss materials which were described by complex dielectric permittivities.

References

1. **Haberland L.** Why is a higher biological relevance attached to importance of pulsed signals? FGH-Newsletter. – 2005. – No 2. – P. 18–21.
2. **Adair E. R., Mylacraine K. S., Cobb B. L.** Partial-body exposure of human volunteers to 2450 MHz pulsed or CW fields provokes similar thermoregulatory responses // Bioelectromagnetics. – 2001. – Vol. 22, No 4. – P. 246–250.
3. **Pakhomov A. G., Doyle J., Stuck B. E., Murphy M. R.** Effects of high power microwave pulses on synaptic transmission and long term potentiation in hippocampus // Bioelectromagnetics. – 2003. – Vol. 24, No 3. – P. 174–181.
4. **Sanders A. P., Joines W. T, Allis J. W.** Effects of continuous-wave, pulsed, and sinusoidal-amplitude-modulated microwaves on brain energy metabolism // Bioelectromagnetics. – 1985. – Vol. 6, No 1. – P. 89–97.
5. **Huber R., Treyer V., Schuderer J., Berthold T., Buck A., Kuster N., Landolt H. P., Achermann P.** Exposure to pulse-modulated radio frequency electromagnetic fields affects regional cerebral blood flow // European Journal of Neuroscience. – 2005. – Vol. 21, No 4. – P. 1000–1006.
6. **Hinrikus H., Parts M., Lass J., Tuulik V.** Changes in human EEG caused by low level modulated microwave stimulation // Bioelectromagnetics. – 2004. – Vol. 25, No 6. – P. 431–440.
7. **Maier R., Greter S. E., Maier N.** Effects of pulsed electromagnetic fields on cognitive processes – a pilot study

- on pulsed field interference with cognitive regeneration // *Acta Neurologica Scandinavica* – 2004. – Vol. 110, No 1. – P. 46–52.
8. **Moore S. K.** Electronic implants and electromagnetic pulses // *IEEE Spectrum*. – 2006. – Vol. 43, No 3. – P. 19–25.
 9. *New fronts in medical device technology* ed. **Rosen A.** and **Rosen H. D.** – New York: John Wiley & Sons Pb., 1995. – 364 p.
 10. **Beason R. C., Semm P.** Responses of neurons to an amplitude modulated microwave stimulus // *Neuroscience Letters*. Elsevier. – 2002. – Vol. 333, No 3. – P. 175–178.
 11. **Nickelson L., Asmontas S., Shugurov V., Martavičius R., Malisauskas V.** SIE method of analysing microwave fields of a 3D heart model // *J. of Electromag. Waves and Appl.* – 2006. – Vol. 20, No 2. – P. 193–206.
 12. **Nickelson L., Ašmontas S., Mališauskas V., Martavičius R., Engelson V.** An Electrodynamical analysis of a model heart // *Electronics and Electrical Engineering*. ISSN 1392–1215. – Kaunas: Technologija, 2005. – No. 7(63). – P. 57–61 (in Lithuanian)
 13. **Knisevskaja(Nickelson) L., Engelson V., Berggren K.-F.** Accurate numerical method for calculating the diffraction characteristics of a human heart model // *Electronics and Electrical Engineering*. ISSN 1392–1215. – Kaunas: Technologija, 2003. – No. 1(43). – P. 13–16.
 14. **Bertašienė Z., Blužas J., Braždžionytė J., Vainoras A., Žaliūnas R.** Computerised stress – Test: usual or new derivative electrocardiographic variables. // *Electronics and Electrical Engineering*. ISSN 1392–1215. – Kaunas: Technologija, 2004. – No. 3 (52). – P. 63–67.
 15. **Beleckij A. J., Babak V. P.** The determined signals and spectrums. – Kiev: “KIT” Publishers (ISBN 966-96166-0-3). – 2002. – 502 p. (in Russian)
 16. **Nickelson L., Shugurov V.** Singular integral equations’ methods for the analysis of microwave structures. – Leiden–Boston: VSP Brill Academic Publishers (ISBN 90-6764-410-2). – 2005. – 348 p.
 17. **Gabriel S., Lau R. W. and Gabriel C.** The Dielectric properties of biological tissues // *Phys. Med. Biol.* – 1996. – Vol. 41. – P. 2251–2293.
 18. **Alison J. M., Sheppard R. J.** Dielectric properties of human blood at microwave frequencies // *Phys. Med. Biol.* – 1993. – Vol. 38. – P. 971–978.

Submitted for publication 2006 05 25

L. Nickelson, S. Asmontas, R. Martavičius, V. Engelson. Microwave Pulse Propagation inside a 3D Heart Model // Electronics and Electrical Engineering. – Kaunas: Technologija, 2006. – No. 8(72). – P. 5–10.

The electrodynamically rigorous solution of Maxwell’s equations related to the microwave pulse propagation inside a three-dimension heart model is presented in this article. The boundary problem was solved by using the singular integral equations’ method. The carrier microwave frequency is 10 GHz. The modulating signals are triangular and rectangular video pulses with the on-off time ratio equal to 3 and 30 for each of pulses. The model heart was limited by a non-coordinate shape surface and it consisted of two different size cavities. The heart cavities were schematic images of the left and right atriums and ventricles. In our calculations the cavities were filled with blood and the walls of the heart consisted of myocardium tissue. The microwave electric field distributions was analysed at three longitudinal cross-sections of the heart model. It is shown that the microwave electric field distribution inside of the heart model most notably depends on the on-off time ratio and form of modulating video pulses.

Ill. 5, bibl. 18 (in English; summaries in English, Russian and Lithuanian).

Л. Никельсон, С. Ашмонтас, Р. Мартавичюс, В. Энгельсон. Распространение микроволновых импульсов в модели сердца // Электроника и электротехника. – Каунас: Технология, 2006. – № 8(72). – С. 5–10.

Приведено электродинамически строгое решение уравнений Максвелла для краевой задачи о распространении микроволнового импульса в трехмерной модели сердца. Краевая задача решена методом сингулярных интегральных уравнений. Несущая частота микроволнового сигнала соответствовала 10 ГГц, модулирующими сигналами служили треугольный и прямоугольный видеоимпульсы со скважностями 3 и 30 каждый из них. Модель сердца ограничена поверхностью сложной формы и содержит внутри две полости, являющиеся аналогами левого и правого предсердий и желудочков сердца. В расчетах полагалось, что эти полости заполнены средой с электрофизическими параметрами крови. Среда, заполняющая остальной объем модели, имеет параметры мышцы сердца – миокарда. Проанализированы распределения микроволнового электрического поля в трех продольных сечениях модели сердца. Показано, что распределение микроволнового электрического поля внутри сердца зависит от скважности и формы модулирующих импульсов. Ил. 5, библи. 18 (на английском языке; рефераты на английском, русском и литовском яз.).

L. Nickelson, S. Ašmontas, R. Martavičius, V. Engelson. Mikrobangų impulsų sklidimas širdies modelyje // Elektronika ir elektrotechnika. – Kaunas: Technologija, 2006. – No. 8(72). – P. 5–10.

Pateiktas elektrodinamiškai griežtas Maxwell’o lygčių kraštinio uždavinio sprendimas, skirtas mikrobangų impulsų sklidimui trimačiame širdies modelyje tirti. Kraštiniam uždaviniui spręsti panaudotas singuliarinių integralinių lygčių metodas. Mikrobangų nešlio dažnis lygus 10 GHz. Jis moduluojamas trikampiiais arba stačiakampiais impulsais, kurių rėtis gali būti 3 arba 30. Širdies modelis yra sudėtingos formos paviršius, o jo viduje yra dvi skirtingų matmenų ir formos ertmės, analogiškos širdies kairiajam ir dešiniajam prieširdžiams bei skilveliams. Skaičiuojant laikoma, kad šias ertmes užpildo terpė, turinti elektrofizikinių kraujo parametrų vertes. Visą kitą modelio tūrį užimanti terpė turi širdies raumens – miokardo parametrų vertes. Ištirtas mikrobangų elektrinio lauko pasiskirstymas trijuose išilginiuose modelio pjūviuose. Įrodyta, kad elektrinio lauko pasiskirstymas širdies viduje priklauso nuo moduluojančiojo impulso formos ir jų rėčio. Il. 5, bibl. 18 (anglų kalba; santraukos anglų, rusų ir lietuvių k.).

DOI: 10.5755/j02.eie.10779